IEEE Access
Multidisciplinary | Rapid Review | Open Access Journal

Received November 17, 2020, accepted December 16, 2020, date of publication December 25, 2020,
date of current version January 5, 2021.

Digital Object Identifier 10.1109/ACCESS.2020.3047457

A Fully Coupled Electromagnetic Irradiation, Heat and Mass Transfer Model of Microwave Heating on Concrete

WEI WEI, ZHU-SHAN SHAO, WEN-WEN CHEN, PENG-JU ZHANG, AND YUAN YUAN
School of Civil Engineering, Xi'an University of Architecture & Technology, Xi'an 710055, China
Shaanxi Key Laboratory of Geotechnical and Underground Space Engineering, Xi'an 710055, China

Corresponding author: Zhu-Shan Shao (shaozhushan@xauat.edu.cn)

This work was supported in part by the National Natural Science Foundation of China under Grant 11872287, and in part by the Found of Shaanxi Key Research and Development Program under Grant 2019ZDLGY01-10.

ABSTRACT Due to the potential for significant process benefit, microwave assisted concrete recycling is highlighted by many scholars and engineers over the world recently. In this paper, a multi-field model is established to simulate the microwave heating process of concrete specimen with single-particle aggregate by using of COMSOL Multiphysics. The validation of this model is verified by comparison with temperature from experiment. Mechanical properties of aggregate-mortar interface during microwave heating process was experimentally investigated. Electric, temperature, stress field evolution and moisture transformation during microwave heating process are discussed in detail. Temperature and stress gradient at mortar-aggregate interface influenced by microwave heating power, frequency and duration are analyzed and graphically presented, which are the dominant factors to achieve the interface debonding. Based on the comparison between concrete absorbed energy and temperature variation, energy efficiency for microwave heating concrete is also briefly discussed. Results of this investigation could provide a multi-field understanding for the microwave treatment on concrete.

INDEX TERMS Microwave heating, concrete recycling, multi-field simulation, interface debonding.

NOMENCLATURE

μ_r	relative permeability (N/A2),
E	electric field intensity (V/m)
ε_r	relative permittivity
j	imaginary unit
σ	electrical conductivity (S/m)
ω	angular frequency (Hz)
T	temperature (K)
μ_0	permeability of free space ($4\pi \cdot$10-7 H/m)
k	solid thermal conductivity (W/(m2·K))
k_{eff}	effective thermal conductivity (W/(m2·K))
kc	mass transfer coefficient
Ri	molar production constant (J/(mol·K))
Di	diffusion coefficient (m2/s)
ε_0	permittivity of free space (8.85 × 10.12 F/m).
k_0^2	wave number in the vacuum
c'	speed of light in vacuum (m/s)
ρ	density (kg/m3)
C_p	specific heat capacity (J/kg/K)
u	velocity field (m/s)
Qted	heat source (W/m3)
q	heat flux (W/m2)
$(\rho C_p)_{eff}$	effective volumetric heat capacity at constant pressure (J/m3K)
c_i	concentration of species (mol/m3)
E	electric field (V/m)
$\mathbf{J}_i$	diffusive flux vector
H	magnetic field intensity (A/m)

The associate editor coordinating the review of this manuscript and approving it for publication was Michele Magno.

I. INTRODUCTION

Microwave is an electromagnetic radiation with frequencies varies from 300MHz to 300GHz, which showed great potential in industrial and scientific practical applications [1]–[5]. Due to its potential for significant process benefit, the recent interest in microwave processing of materials is highlighted

by many research groups all over the world. Compared with traditional heating methods, microwave heating offers a rapid, volumetric and high-safety heating process. Experts generally agree that it is a green, clean, efficient and sustainable energy supply. Recently, microwave heating has been applied on concrete and rock processing, such as microwave assisted concrete curing, rock and concrete breaking, drilling, material pre-heating and concrete recycling.

The development of construction industry results in high consumption of concrete and then huge volume of Construction and Demolition (C&D) waste worldwide. Many countries are currently facing shortage of natural aggregates. The utilization of recycled concrete aggregate (RCA) has great significance in realizing the sustainable development of the construction industry. How to separate the mortar and aggregate effectively is the critical issue for high-quality aggregate recycling. The properties of mortar, aggregate and their interface under different treatment methods is the priority for the effective recycling.

Conventional heating approach could separate mortar and aggregate under certain temperature. Within conventional thermal separation, aggregates are heated to the temperature varies from 300°C to 600°C. Generally, several hours are needed to reach the required temperature through the conventional heating cavity, with high energy consumed. In addition, the high temperature under long heating duration may lead to the performance degradation of recycled aggregate compared with the natural aggregate. As a most common separation method, the principle of mechanical methods for mortar and aggregate separation is the rubbing and impact forces to separate the adhering mortar. High dust and noise pollution were generated, and relatively high energy was consumed, secondary pollution will be produced.

Recently, microwave heating technique has be considered as the potential solution for effective recycle method of concrete aggregate even when the materials was only subjected to low heating energy [6]–[9]. Microwave heating represents the transfer of electromagnetic energy to thermal energy [10]–[13]. One principle of microwave effective heating is due to the volumetric heating process subjected to concrete material, the materials under microwave irradiation could be heated within few minutes [14]–[18]. Another feature is the selective heating property of microwave [19]–[23]. When concrete is irradiated under microwave, mortar, aggregate and water could be heated under electromagnetic field. Energy conversion and transfer of mortar, aggregate and surroundings environment would happen during the whole heating process. The heating effect is affected by dielectric and thermal properties of mortar and different types of aggregate, and also by the electric and magnetic field distribution within the heating cavity. The response of mortar and aggregate within concrete towards microwave heating are largely different. The difference of materials' response lead to different electromagnetic and thermal field, resulting in the thermal stresses gradients between materials [24]–[27]. Precious research indicated that stress and strain of mortar, aggregate and the interface are continuous changed during heating period. The internal stresses may induce the fracture especially at the interface of aggregate and mortar [28].

Many experiments have already indicated that microwave can induce severe damage of concrete. Microwave processing could improve the comminution properties and liberation of both aggregate and cement. Particularly, researches proved that boundary cracks of mortar and aggregate would form after microwave treatment, the intergranular crack, in other words [29]–[31]. Research demonstrated that microwave treatment pre-treatment positively affects aggregate liberation and cement matrix removal. Due to its heating characteristic, even when concrete under short heating time and low microwave power level, there are still crack generated at the boundary of mortar and aggregate. Considering the aspect of both aggregate effective utilization and energy consumption, microwave heating assist aggregate recycling could be regarded as a potential and prospective technique for future application. However, the electromagnetic, thermal and mechanical evolution could not be predicted or quantitatively described only during the experimental investigation. The experimental research could only provide the macro separation result, the content mortar adhesion, strength, failure mode, for example.

In last few years, numerical simulation researches were achieved to give an insight into the complex multi-field coupling of microwave treatment process [32]–[37]. As powerful software, COMSOL Multiphysics could model microwave heating by coupling electromagnetic, solid heating, solid mechanics and mass transfer modules. Hong *et al.* [38] simulated the heating behavior of coal under microwave irradiation by COMSOL Multiphysics. The effects of microwave frequency, microwave power and sample position were demonstrated. Similarly, Lin *et al.* [39] analyzed the sensitivity on microwave heating of coal, with several influence parameters incorporated in the model. However, the mass transfer process was neglected in the analysis. The moisture content, moisture distribution and heat evaporation were ignored, which does not present the actual heating circumstance [40]. Fewer investigations were made subject to the multi-field problem of concrete under microwave treatment. There are many attempts to understand the response of concrete under the influence of an electromagnetic field. The phenomena associated with the multi-field heating processing are less understood. The heat and mass transfer process of concrete under electromagnetic field has to be studied to give a deeper insight into the microwave heating on both macro and micro level. As the good microwave absorbed material, the existence of water could affect the heating results effectively. When the heating temperature reached a certain level, the form variations of water could influence the heating phenomenon. The conversion and transformation of this moisture would have an impact on the heating result. During the microwave heating concrete, only the polar molecule with high dielectric properties absorbed microwave energy, leading to the temperature increase. The polar molecule rotated

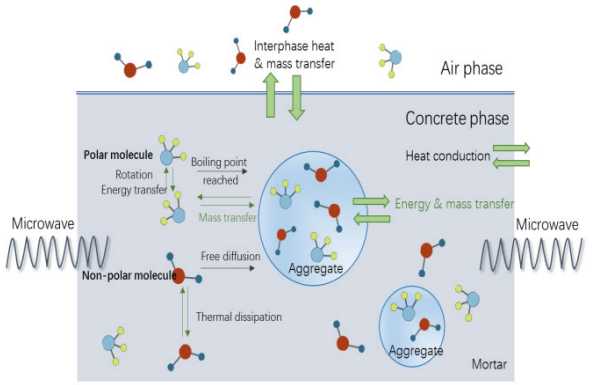

FIGURE 1. Energy, heat and mass transfer of concrete under microwave irradiation.

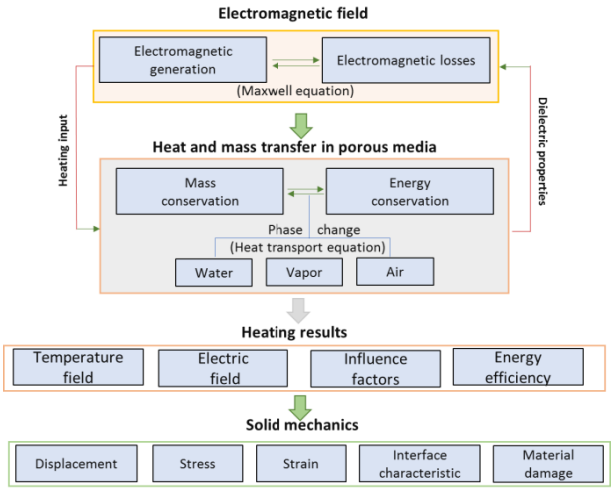

FIGURE 2. Research approach.

due to the microwave energy, clustering together as vapor bubbles when the temperature reached the boiling point, transferring from concrete phase to surrounding air phase, shown in Fig.1. The formation process of bubbles leads to the energy and mass transfer process in concrete. When the bubbles transfer from concrete to air phase, the heat and mass transfer process happened. The mass transfer process is influenced by the heat transfer circumstance, and vice versa. Therefore, the further understanding of moisture variation within concrete under microwave irradiation is the primary consideration. Additionally, the mechanical field simulation is needed for the study of mechanical mechanism during the heating process. The stress and stain lead to interface debonding are needed to be clarified. The energy efficiency of heating process needs to be considered for the possible effective aggregate recycling.

The aim of current research is to present a 3D simulation to study the multi-field coupling process of concrete under microwave treatment. Multi-field simulation for microwave heating of concrete is firstly performed and verified by experimental temperature results. A simplified concrete model is employed to investigate the response of aggregate and mortar under microwave irradiation and also the interaction between the two materials. Although the real shape, size and location of aggregate could not represent in the simplified model, the heating response of mortar and aggregate could be captured, and the microwave heating mechanism could be investigated. Push-out tests are conducted after microwave heating process to investigate the interface the mechanical behavior of aggregate-mortar interface after microwave heating. Four physical fields are used in numerical simulation, the mechanical field, electromagnetic field, thermal field and mass transfer field to illustrate the complex and more practical multi-field heating process of concrete.

The microwave was generated through the electromagnetic generation and electromagnetic losses. The electric, thermal and stress field are analyzed firstly, shown in Fig.2.The moisture evolution and phase change of sample during heating process and the internal mechanism are discussed. The influence factors relating to the microwave processing efficiency are illustrated, including microwave heating frequency, power and time. The heating efficiency is studied quantitatively subjected to different microwave frequency. Particularly, the mortar-aggregate interface properties such as temperature difference, stress variation and mutation under microwave heating are discussed subject to the interface debonding.

II. MULTI-FIELD SIMULATION

A. METHODOLOGY

The COMSOL Multiphysics is employed to simulate the multi-field heating process in mortar-granite concrete under microwave irradiation. With COMSOL Multiphysics, conventional models for only one circumstance of physics could be easily extended into multiphysics models, which could solve the multi-field problems. COMSOL Multiphysics can model microwave heating by coupling electromagnetic and heat transfer physics. The software solves the numerical models using finite element method (FEM).

B. GEOMETRY OF MULTI-FIELD MODEL

The model geometry is established based on the microwave oven model in COMSOL Multiphysics application gallery, as shown in Fig. 3. Heating sample was placed at the bottom center of oven. Microwave sources were transfer through the waveguide into microwave oven. The microwave oven and waveguide are filled with air. The concrete was simplified as a single aggregate concrete, which was composed by granite and mortar. Granite was chosen as the typical kind of aggregate. Granite and mortar were acted as the inclusion and host part, respectively. The diameters of heating cavity, waveguide and sample were tabulated in Table 1. The heat and mass transfer process and the mechanical field evolution for granite and mortar phases could be both simulated through the model. Particularly, the heating characteristic of interface between granite and mortar could be clearly observed.

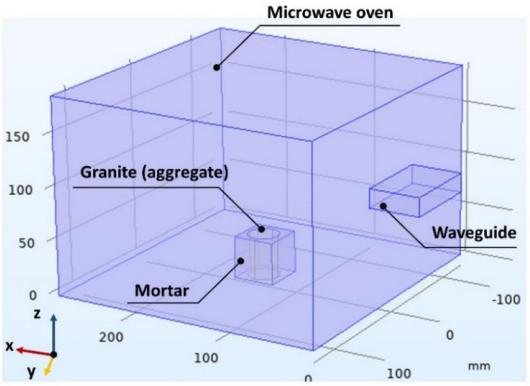

FIGURE 3. Geometry of heating model.

TABLE 1. Model parameters.

	Width (mm)	Depth (mm)	Height (mm)	Radius (mm)
Microwave oven	267	270	188	-
Mortar	40	40	40	
Granite	40	-	-	15

TABLE 2. Thermo-physical properties of mortar and granite and the initial conditions.

Descriptions	Value	Reference
Air moisture concentration	0.05[mol/m^3]	
Initial temperature of sample and air	298.15 [K]	
Granite density	2609 [kg/ m^3]	[41]
Mortar density	2430 [kg/ m^3]	[42]
Specific heat capacity of granite	800 (J/kg K)	[43]
Specific heat capacity of mortar	1600(J/kg K)	[43]
Thermal conductivity	2.55 (W/m K)	[44]
Thermal conductivity of mortar	0.98 (W/m K)	[45]
Thermal expansion coefficient of granite	7.1×10-6 (1/ K)	[46]
Thermal expansion coefficient of mortar	19×10-6 (1/ K)	[43]
Relative permittivity of granite	3-0.1j	Experiments
Relative permittivity of mortar	2-5j	Experiments

The thermo-physical and dielectric properties of mortar and granite are considered as a constant under various temperature. The properties of mortar and granite were tableted in Table 2, which was obtained from related literature. Initial temperature of sample and air were 298.15 K, that is 25 °C.

Mesh size and quality has important impact on the accuracy of the finite element analysis. The model is built with ''fine element'' size, and the maximum mesh size was set to 1/5th of the microwave wavelength. The quality evaluation of mesh element is shown in Fig.4. There are 27726 elements in the model, the average mesh quality is 0.66, confirming that the elements are regular, and the model is reliable.

C. ASSUMPTIONS

In this paper, several assumptions were considered within the model during the analysis to simplify the problem to some extent, listed as below;

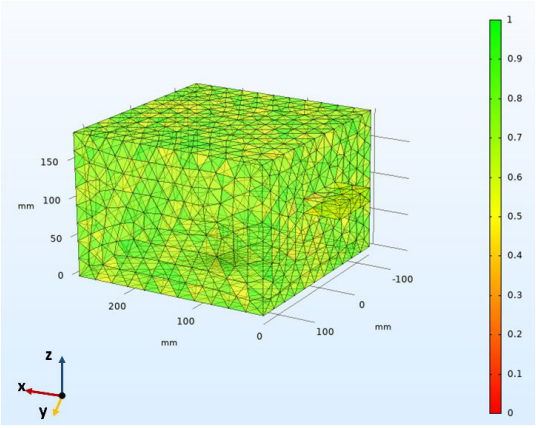

FIGURE 4. Model element and quality evaluation.

a) The walls of the oven and the waveguide are perfectly conducting;

b) The initial temperature distribution of sample and air are homogeneous;

c) Granite and mortar are considered as homogeneous porous media;

d) Chemical reaction is not considered in the heating process.

D. GOVERNING MECHANICS

1) ELECTROMAGNETIC FIELD

The electromagnetic is governed by the Maxwell's equation. The Maxwell's equations describe how electric and magnetic fields propagate, interact, and how they are influenced by objects. Effects of many electromagnetic characteristics are considered in these equations, the electric field intensity **E**, the electric displacement or electric flux density **D**, the magnetic field intensity **H**, the magnetic flux density **B**, the current density **J**.

The governing equation is given as:

$$\nabla \times \mu_r^{-1} (\nabla \times \boldsymbol{E}) - k_0^2 \left(\varepsilon_r - \frac{j\sigma}{\omega \varepsilon_0} \right) \boldsymbol{E} = 0 \qquad (1)$$

where μ_r is the relative permeability (N/A^2), $\boldsymbol{E}$ denotes the electric field intensity (V/m), ε_r represents relative permittivity, j is imaginary unit, σ is the electrical conductivity (S/m), ω represents the angular frequency and ε_0 is the permittivity of free space (8.85×10^{-12} F/m).

2) TEMPERATURE FIELD

The heat generated by microwave heating need to be coupled into heat transfer equation in concrete. Based on Fourier's energy balance equation within the area of microwave oven and the waveguide, heat transfer is given by the following equation:

$$\rho C_p \boldsymbol{u} \cdot \nabla T + \nabla \cdot \boldsymbol{q} = \boldsymbol{Q} + \boldsymbol{Q}_{ted} \qquad (2)$$

where Q_{ted} is the microwave heat source (W/m^3), ρ is the density (kg/m^3), C_p is the specific heat capacity (J/kg/K), u is

the velocity field (m/s), T is the temperature (K), Q represents the heat of moisture vaporization; heat flux q is express as:

$$\boldsymbol{q} = -k\nabla T \tag{3}$$

where k is the solid thermal conductivity (W/(m^2·K)).

For the heating sample mortar and granite, the moisture content within these porous media could affect the heat transfer process, the heat transfer equation is expressed as:

$$\left(\rho C_p\right)_{eff} \frac{\partial T}{\partial t} \rho C_p \boldsymbol{u} \cdot \nabla T + \nabla \cdot \boldsymbol{q} = Q \tag{4}$$

$$\boldsymbol{q} = -k_{eff} \nabla T \tag{5}$$

$$k_{eff} = \theta_p k_p + \left(1 - \theta_p\right) k + k_{disp} \tag{6}$$

where ρ is the fluid density (kg/m^3), C_p is the fluid specific heat capacity (J/kg/K), $\left(\rho C_p\right)_{eff}$ is the effective volumetric heat capacity at constant pressure (J/m^{3}K), q is the conductive heat flux (W/m^2). u is the fluid velocity field(m/s), k_{eff} is the effective thermal conductivity (W/(m^2 · K)), Q represent the microwave heat source (W/m^3).

3) DISPLACEMENT FIELD

The stress, strain, displacements and velocity of concrete under microwave heating was induced by temperature variation, moisture transfer, and the material mechanical properties.

For example, the strains of sample during the heating process was given by:

$$\varepsilon_{inel} = \varepsilon_0 + \varepsilon_{ex} + \varepsilon_{th} + \varepsilon_{hs} + \varepsilon_{pl} + \varepsilon_{vp} + \varepsilon_{cr} \tag{7}$$

where $\varepsilon_0, \varepsilon_{ex}, \varepsilon_{th}, \varepsilon_{hs}, \varepsilon_{pl}, \varepsilon_{vp}, \varepsilon_{cr}$ are the initial strain, external strain, thermal strain, hygroscopic strain induced by mass transfer, plastic strain, viscoplastic strain and creep strain, respectively. The strain composition and variation could present the multi-field coupling of the heating process clearly.

A fixed constraint node adds at the bottom surface of mortar and granite, which act as a condition that makes the geometric entity fixed. It means that the displacements are zero in all directions, that is $\mathbf{u} = 0$.

4) MASS TRANSFER

As the good microwave absorbed material, the existence of water could affect the heating results effectively. When the heating temperature reached a certain level, the form and distribution of moisture will be changed, which could influence the heating phenomenon. The conversion and transformation of this moisture would have an impact on the heating result. Thus, the mass transfer process should be considered. The mass transfer solved in the porous media in granite and mortar expressed as:

$$\nabla \cdot \mathbf{J}_i + \mathbf{u} \cdot \nabla c_i = R_i \tag{8}$$

where c_i denotes the concentration of species (mol/m^3), $\mathbf{u}$ is the fluid velocity (m/s), R_i is the molar production constant (J/(mol·K)), $\mathbf{J}_i$ is the diffusive flux vector, given as:

$$\mathbf{J}_i = -D_i \cdot \nabla c_i \tag{9}$$

where D_i is the diffusion coefficient (m^2/s)

5) BOUNDARY CONDITION

During the heating process, the impedance boundary condition was used to define the walls of waveguide and microwave oven and the equation is given by:

$$\sqrt{\frac{\mu_0 \mu_r}{\varepsilon_0 \varepsilon_r - j\sigma/\omega}} \boldsymbol{n} \times \boldsymbol{H} + \boldsymbol{E} - (\boldsymbol{n} \cdot \boldsymbol{E})\boldsymbol{n} = (\boldsymbol{n} \cdot \boldsymbol{E_s})\boldsymbol{n} - \boldsymbol{E_s} \tag{10}$$

where μ_0 is the permeability of free space, $\mathbf{H}$ is the magnetic field intensity (A/m), $\mathbf{E_s}$ denotes electric field source;

The waveguide and heating oven boundary are described as perfect magnetic conductor as:

$$\mathbf{n} \times \mathbf{H} = \mathbf{0} \tag{11}$$

The port boundary was defined as a rectangular input, the microwave was input through the port boundary, the scattering parameters is described as:

$$S = \frac{\int_{port} (\mathbf{E} - \mathbf{E}_1) \cdot \mathbf{E}_1}{\int_{port} \mathbf{E}_1 \cdot \mathbf{E}_1} \tag{12}$$

where $\mathbf{E}$ is the computed electric field, $\mathbf{E_1}$ is the electric field in port 1;

In the thermal field, the boundary of sample is defined as thermal insulation boundary condition, which means that the temperature was continuous at the boundary, that is the temperature on one side of the boundary must equal the temperature on the other side;

$$\mathbf{n} \cdot (-k\nabla T) = 0 \tag{13}$$

In the mass transfer field, convention is applied to the sample, given as

$$-\mathbf{n} \cdot (-D\nabla c) = J_0 \tag{14}$$

$$J_0 = k(c_b - c) \tag{15}$$

where D denotes the moisture diffusion coefficient in the sample, c_b is the air moisture concentration, k_c refers to the mass transfer coefficient.

The bottom face of sample is defined as no flux boundary condition, that is, $J_0 = 0$.

III. EXPERIMENTAL TEST

Experiment was carried out in an industrial multimode microwave heating system (CY-MU1000C-L) in the research, which was manufactured by CHANGEMW Microwave Technology Development Co., Ltd., China. The incident microwave power is tunable from 0 to 6000W and the water-cooled magnetron operated at a frequency of 2.45GHz. Microwave input power and exposure time are controlled by the Programmable Logic Controller (PLC) and touch screen, as shown in Fig.5. The heating temperature, duration and power could be set before the heating process. The dimension of heating cavity is 110 × 110×110 mm, enclosed by the thermal insulation material. The heating temperatures were monitored by thermocouple during the heating process.

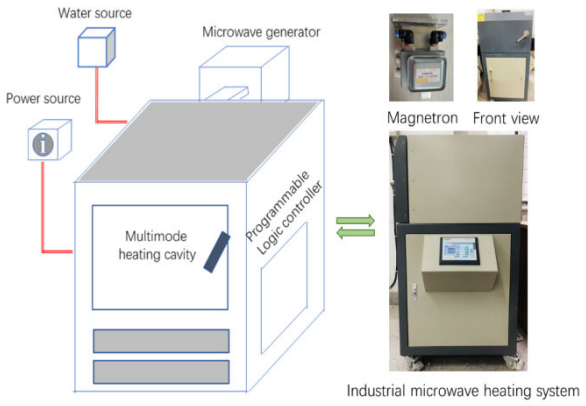

FIGURE 5. Multi-mode industrial microwave heating system.

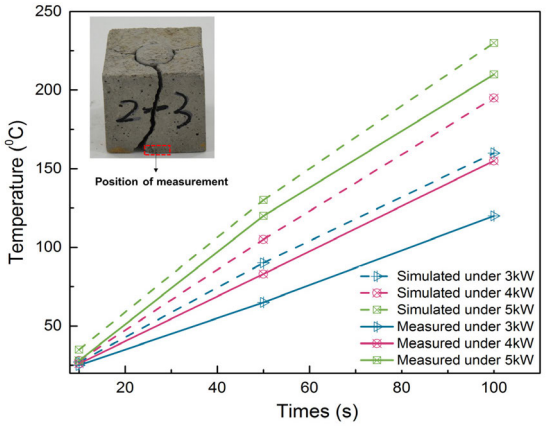

FIGURE 6. Experimental measured and simulated temperature of concrete.

Mortar-aggregate specimens are designed as cubes, with dimensions of 40mm×40mm×40mm designed, which are the same with the simulated model. The concretes with single aggregate were designed to represent the connection between the aggregate and mortar. The concrete sample is a simplified model of normal concrete, consisting of an aggregate and mortar with the strength grade of M30. The cylinder aggregate is in the center of specimen, the diameter is 15mm and the height is 40mm. PO 42.5 grade ordinary Portland cement was used in this study. The compressive strength of mortar was 35.2MPa. The fine aggregate was taken from Weihe River, Xi'an, China. The fineness modulus was 2.6, and its physical and mechanical properties met the ⟪General Concrete Sand and Stone Quality Standards and Test Methods⟫ (JGJ52-2007) requirements. The mortar was filled in mould around the aggregate on a vibrating table. After 28 days of standard water curing at a temperature of 25 °C, the samples were ready to be used in both microwave heating experiments. The typical small area for temperature measurement was presented. The microwave heating effect of this model was verified through comparing to the microwave heating experiments. The comparison of experimental and simulation results is shown in Fig.6.

It is shown that the simulation results almost agree well with the experimental results except for minor temperature difference. The differences may due to the assumptions of the simulation model and the limitation of experiments. For example, the frequency in experiments may varied or fluctuated. The relative permittivity, moisture conductivity and mass transfer coefficient are set as constant in the simulation model, which could lead to the difference of simulation and experiment result. In addition, the homogeneity assumption of components of concrete could lead to the deviation of simulation results. The experimental validation proved that the numerical model is considered accurate enough to perform further simulations.

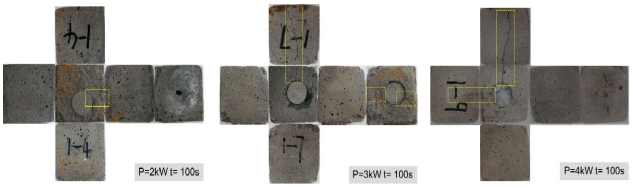

FIGURE 7. Cracks formation in mortar-granite sample under microwave treatment.

The fracturing effect of microwave treatment and the expanded view of cuboidal mortar-granite sample are shown in Fig. 7. The cracks formed after the microwave heating under 2kW for 100s. The crack started from the interface of mortar and granite aggregate, extending towards the mortar matrix. The cracks penetrated to the three side surfaces perpendicular to the end surface. Some mortars were fall off from the sample near the aggregate, which may due to the thermal stress concentration and temperature difference around the mortar-aggregate interface. With the increment of heating time and microwave power, the cracks occurred in samples enlarged, leading to the total debonding of aggregate and mortar. Under the microwave heating, the separation cannot be realized by the temperature rise alone, the expansion must take place at the interfacial layer. The experimental results proved the potential of microwave assisted concrete-aggregate recycling.

Then the meso-mechanical laboratory push-out test was carried out to identify the mortar- aggregate interface properties after microwave irradiation. The push-out tests were undertaken with an electro-hydraulic servo universal testing machine WAW-1000. Aggregate push-out tests were conducted by using the set-up are displayed in Fig.8. The load was applied on the center point of aggregate. Interfacial bond strength, τ was obtained by dividing the maximum load (MPa), P_{max} by the nominal shear area which is given by the product of the circumference of the cylindrical aggregate and the depth, ($\tau = P_{max}/2\pi rL$), where L is the constant length of the cylindrical aggregate as 40 mm and r is the radius as 15 mm. Push-out test were conducted under different conditions of microwave heating process to investigate the interface the mechanical behavior of aggregate-mortar interface.

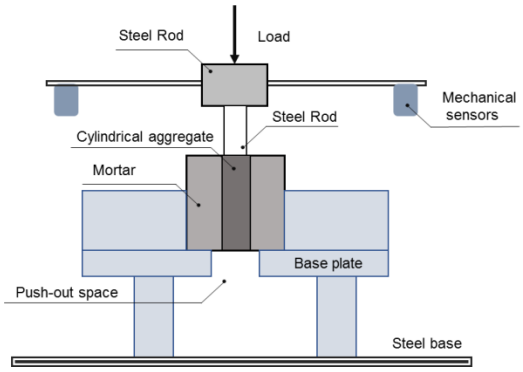

FIGURE 8. General view of the aggregate push-out test set-up.

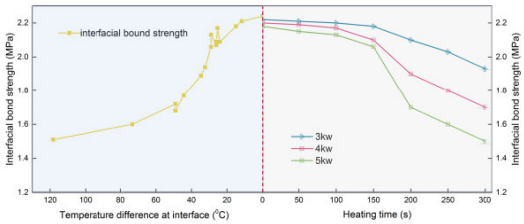

FIGURE 9. Interfacial residual bond strength under different heating time and power.

It could be seen that when the irradiation time was less than 150 seconds, the curve changes very gently, the residual bond strength is basically unchanged compared with the untreated specimens (Fig.9). When the irradiation time reached 150 seconds, the residual bonding strength decrease rapidly, compared with the decrease of bonding strength by only 8.0% at 150s, the bonding strength at 5kW power at 200s is reduced by 32.6%. The curves indicate that under the same irradiation time, increasing the microwave power can significantly reduce the bond strength between aggregate and mortar. From the aspect of temperature difference, it can be clearly seen that the change in bond strength is related to the temperature gradient between aggregate and mortar. Larger temperature difference at interface result in lower interfacial bond strength, which could facilitate the interface debonding of mortar and aggregate [47].

IV. RESULTS AND DISCUSSION

A. ELECTRIC, TEMPERATURE, AND STRESS FIELDS

Microwave generated from waveguide would be reflected continually by the wall of heating cavity. The electromagnetic field was formed unevenly, with heterogeneous-distributed high- energy and low- energy region co-existed. Introduction of concrete redistributes the electric field through the absorption of the microwave energy. Generally, the microwave frequency, sample size and morphology, sample dielectric properties, sample and waveguide's position could affect the distribution and magnitude of electric field. The microwave electric field was attenuation when pass through concrete samples, which was caused by energy transformation.

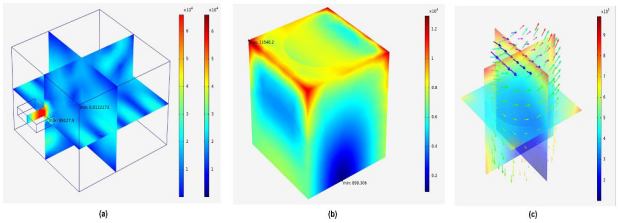

FIGURE 10. Electric field of (a) whole cavity (b) sample (c)granite.

Sample would be heated rapidly in the heating cavity due to the continuous conversion of electromagnetic to thermal energy. As shown in Fig.10, the strongest electric field in the mortar-granite was concentrated at the corner of upper surface of mortar phase under the 1 kW microwave power. The upper part of mortar and granite suffered stronger electric field.

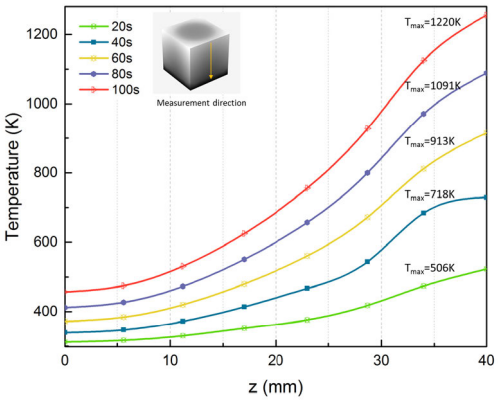

FIGURE 11. Temperature profile along the z-direction.

Initially, the thermal fields are distributed uniformly at the temperature of 298K. A cold spot appeared at the bottom center of the concrete sample. Higher temperature region showed at the center and corner of sample surface in the beginning. As the heating time grows, the region of high-temperature enlarged, while the low-temperature region shrunken. The temperature field distribution along the measurement line were captured with 100s heating time (Fig.11). At the top surface, z=0, the bottom surface z=40. The longer the heating time, the larger temperature difference exhibited, the faster maximum temperature increased. Higher electromagnetic intensity leads to faster polarization effect, resulting in increment of heating temperature and thermal field. The distribution of temperature was corresponded to variation of electromagnetic field.

Fig.12 illustrates the sample's stress field and interfacial stress of mortar and granite under the 1 kW microwave power. To evaluate the mortar, granite and the interface properties, the stress state and deformation within sample are needed. For the whole sample, tensile stress acted as the dominant stress. It can be seen from the cross section across center of both

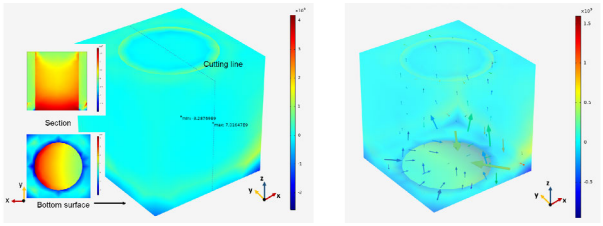

FIGURE 12. (a) Major principal stress of sample (b) Interfacial stress of mortar and granite.

the mortar and granite that there was a marked change of the principal stress at the interface of mortar and granite, which was due to the difference of thermal and mechanics properties of two materials shown in Fig.12 (a). The mechanics condition was beneficial for the possible interface separation. The stress gradients increased with the increment of heating time. The minimum principal stress occurred at the corners of bottom surface of sample because of the definition of boundary conditions. It can be seen that there were shear stress was the dominant stress formed at the boundary of two material Fig.12 (b), contributing to the interface failure.

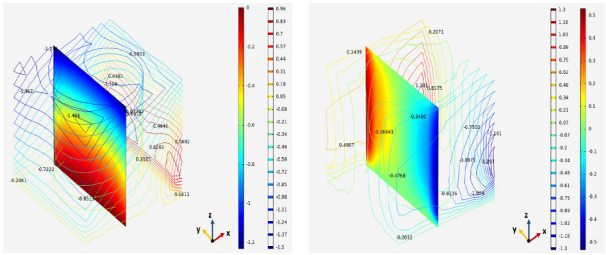

FIGURE 13. (a) x-direction displacement (b) y-direction displacement of sample.

The displacements of two sides of sample in y-direction were symmetrical, shown in Fig.13 (b), which may be due to the homogeneous distribution of electric and thermal field in the y-direction. In x-axis direction, in other words, microwave entry orientation, the displacement of sample's surface was greater. It was interesting that the maximum displacement occurred at the corner of sample, which was closest to the waveguide. The following was the corner at the maximum distance from waveguide, on the diagonal, in other words. The electromagnetic field was aeolotropic within the heating cavity. Microwave transferred from waveguide reflected continually to the heating cavity, the part would be absorbed by samples, which were no longer uniformly distributed as beginning. The position of waveguide and sample could influence the distribution of the electromagnetic field, leading to the variation of mechanical properties of concrete sample.

Temperature, electric and stress field within mortar and aggregate especially at the interface under heating power of 1kW were shown in Fig.14. The variations of electric, temperature and stress field were interrelated and interacted. It could be found that within the concrete, electric field

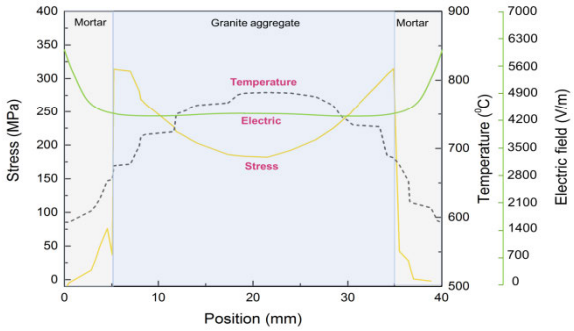

FIGURE 14. Temperature, electric and stress field within mortar and aggregate.

attenuation was occurred. As the microwave absorber, when microwave propagated through the concrete, electromagnetic energy was transformed into heat energy, presenting as the electric field attenuation, resulting in temperature increase within concrete. There was a sharp increase of temperature at the interface. The different dielectric properties of mortar and aggregate leads to different heating rate and temperature results under microwave irradiation, resulting in the temperature gradient. The temperature gradient leads to corresponding stress gradient. The boundary debonding was formed based on the stress variation, which caused by stress difference and thermal expansion. The stress mutation at the interface could facilitate the interface debonding behavior.

B. MOISTURE TRANSFER IN SPECIMEN DURING HEATING PROCESS

Moisture existence and transformation plays an important role in the heating process, while few previous studies analyzed the mass transfer evolution during the heating process. In this model, mass transfer field was collaborated to illustrate the heating process more systematically and accurately. The heat generation induced by electromagnetic losses, water evaporation and heat convection could affect the temperature field evolution within concrete. Moisture exists in two main states within materials, chemically bounded moisture and free moisture in the pores. Free moisture includes the surface absorbed water and interparticle water. When sample was exposed to microwave heating, the moisture state and content will be changed. Free water in the pores occurred when the temperature reached the boiling point. As heating temperature increased, bounded water was released and transformed into steam under sufficient power density, which could decrease the density of sample and influence sample's dielectric properties of materials. And the dielectric properties change could in turn affect the heating results, including the moisture content and distribution. The mechanical properties of mortar and granite under microwave heating directly relate to their dielectric properties, which means that the mechanical properties could be affected by the moisture variation. The nonuniformity temperature distribution lead to the increment of vapor pressure gradient, resulting in the vapor diffusion in concrete and eventually in surrounding

environment. During the process, damage will occur in concrete owing to the gradient of vapor stress and temperature. In addition, the properties of mortar and granite may undergo significant chemical change, with the bond broken and molecular structure changed. Water saturation enhances the liberation of some material particularly while have little effect on others. The heating results for mortar and granite was largely different even they were under almost same water content.

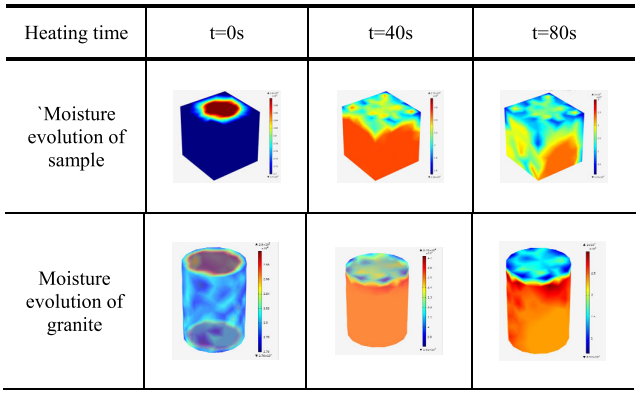

FIGURE 15. Moisture evolution of sample under microwave irradiation.

The moisture content of granite was a little bit higher than that in mortar when t=0s in the initial condition, shown as in Fig.15. A moisture concentration spot was formed at bottom center of the sample initially, which was coincides to the temperature cold spot. The upper part of sample was heated more effectively based on the distribution of electromagnetic field under microwave irradiation. As the increment of heating time and temperature, the moisture content of upper part declined. Within mortar, the area contents higher moisture shrunken with the increase of heating time, while the area within granite remain almost the same as the inclusion. Compared with the moisture distribution within granite, the mortar's surface moisture could be easier evaporated and diffused, with lower moisture content appeared. Generally, the increment of water content in sample can significantly increase the microwave heating rate. In the beginning, the moisture content was distributed uniformly within the sample. With the increment of heating time, moisture content starts to change. With higher content of moisture evaporated, higher heating rate and temperature field presented. It is why less moisture contents remained corresponding to higher temperature presented. Within the conventional heating process, the heat is transferred from the surface towards the center of the material, thus the vapor evaporation was more likely formed on the concrete surface. After a duration of heating process, higher temperature may occur in the inner part of concrete. However, the phenomenon was largely different under microwave irradiation owing to its volumetric heating characteristic. The analysis of water content variation and mass transfer process could provide the reference to evaluate the heating efficiency and predict the following heating process. From the distribution law of water content within the sample, it could be concluded that there existed an interaction effect distribution of moisture field, temperature field and electromagnetic field during the heating process.

C. EFFECT OF MICROWAVE POWER

The variation of maximum and minimum temperatures under different heating time and microwave power were shown in Fig.16. Before the heating process, thermal fields were distributed uniformly throughout the whole heating sample. As the heating time and microwave power grows, the electric intensity and thermal field both increased, the average temperature increased accordingly. The hot spot enlarged, extended deeper towards the sample. The distribution pattern of temperature fields was almost the same. Both the maximum and minimum temperature of sample were occurred in the mortar. The temperature gradients within granite were smaller than that in mortar, which means that the temperature field in granite was more uniformly. Based on the analysis of stress field and displacement of mortar, easier and earlier damage may occur in mortar part. The positions of maximum temperature gradient occurred at the top or side surface of granite, that is the interface of mortar and granite, instead of the interior body of granite.

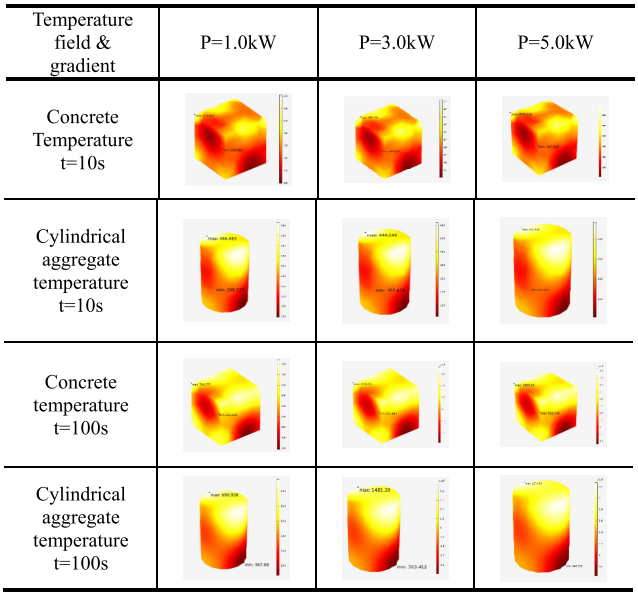

FIGURE 16. Effect of microwave on the sample's temperature field.

Results found that the displacement of surrounding mortar was larger than that of inner granite under the microwave treatment, indicating that the mortar may suffer damage firstly. The displacement of interface granite was selected to analyze the effect of microwave power on sample's deformation. The displacement of interface was caused by the thermal expansion effect of granite and mortar, which was also affect by the stress gradient between materials. It is obvious that higher microwave power lead to larger surface displacement after same heating time (Fig.17). The slope

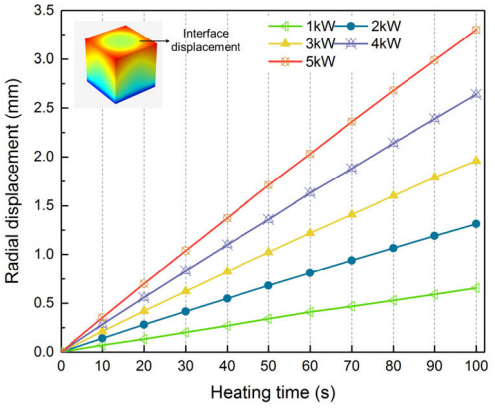

FIGURE 17. Effect of microwave power on granite radial expansion at interface.

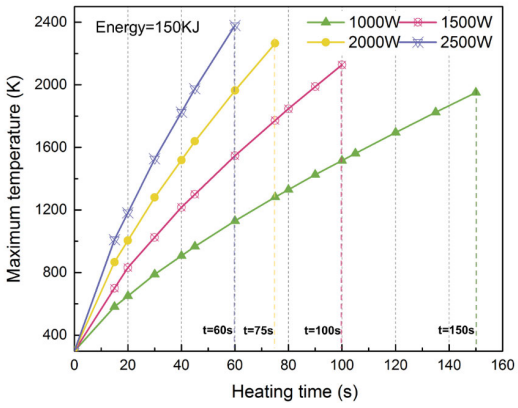

FIGURE 18. Effect of microwave power on maximum temperature.

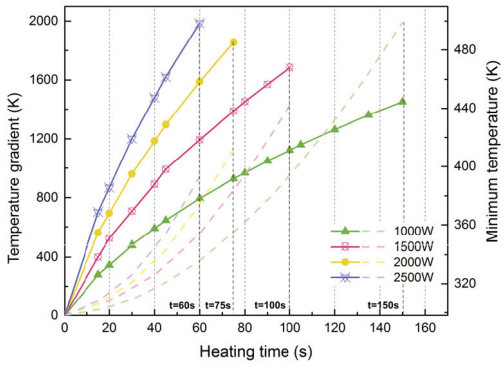

FIGURE 19. Effect of microwave power on minimum temperature and temperature gradient at interface.

the curve indicated that higher power could induce larger deformation per unit time. For the same displacement, less time was needed for higher microwave frequency. It could be seen that under 5kW microwave heating of 100s, the interface displacement has reached 3mm, indicating the interface debonding of mortar and aggregate. There may exist a critical microwave power value for mortar broken while granite keeps intact.

It is obvious that larger power results in larger electric field intensity and higher average temperature. However, during the heating process, heating efficiency should be considered from the standpoint of economic. Heating process hope to achieve the maximum output value with least investment. The heating efficiency is directly relating to the selection of microwave power and heating time, that is, the energy input. Four same energy input with different microwave power were simulated in the model to find out the influence of microwave power under same energy input. Taking energy inputs 150KJ as example, four kinds of combination were employed, 1000W$\times$150s, 1500W$\times$100s, 2000W$\times$75s and 2500W$\times$60s. Maximum temperature occurred when the microwave power was 2500W. Taking temperature 1200K as example, it could be seen that for 2500W's microwave power, only 20s were needed to reach the temperature while for microwave power of 1000W, heating time was extended to about 70s. In other words, higher temperature could be firstly reached within fewer heating time. It was obvious that the slope of 2500W microwave power curve was largest (Fig.18).

The relationship of temperature difference, minimum temperature and heating time was shown in Fig.19, the solid line represent the temperature difference and the dashed line represent the minimum temperature. T_{max} increase with the increment of microwave power while the T_{min} decreased. Under the highest microwave power treatment, the temperature difference reached almost 2000K while the minimum temperature was the lowest compared with other power treatment. In other words, higher microwave power lead to larger temperature difference within the sample. Lower microwave power may result in more homogeneous temperature field. It could be concluded that higher microwave power level combined with shorter heating time may result in higher heating efficiency, with less energy input needed while higher temperature achieved.

D. EFFECT OF MICROWAVE FREQUENCY

Previous researches indicate that the frequency generated by microwave heating system fluctuates during the heating process. When the microwave power source is 2.45GHz, the frequency may vary from 2.40GHz to 2.49GHz with typical chaotic irradiation spectra of magnetrons. In the section, the frequency of 2.41GHz, 2.43GHz, 2.45GHz, 2.47GHz and 2.49GHz were selected to investigate the microwave frequency effect on the heating results.

The thermal and electric field of sample and cross section of mortar and granite after microwave heating after 100s microwave irradiation under same power input was shown in Fig.20. The electric filed was largely affected by microwave heating frequencies. When microwave frequency changed for only 50MHz, the intensity of electric field varied doubled. Different microwave frequencies result in different electric field within the heating cavity and the sample, leading to the difference in the thermal and stress field. The moisture content and distribution were also varied under different heating frequencies. For different microwave heating

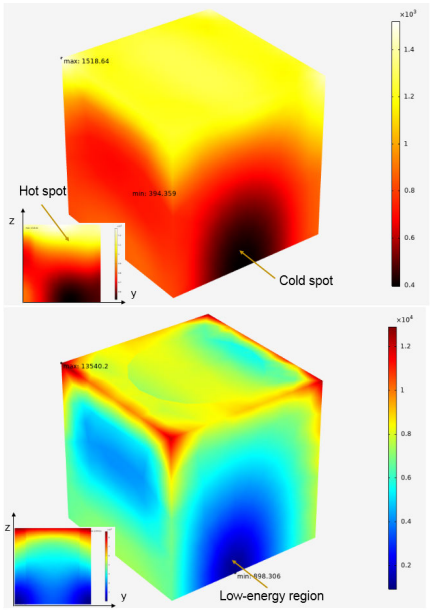

FIGURE 20. Effect of microwave frequency on electric and temperature field (2.45GHz).

frequency, the strongest electric fields were all distributed at the corner of the upper surface. It can be obviously found that the thermal field varies with the change of microwave frequency. The value of maximum and minimum temperature fluctuated under different frequency. The shape and area of temperature cold spot and electric low-energy region were evidently affected by heating frequency.

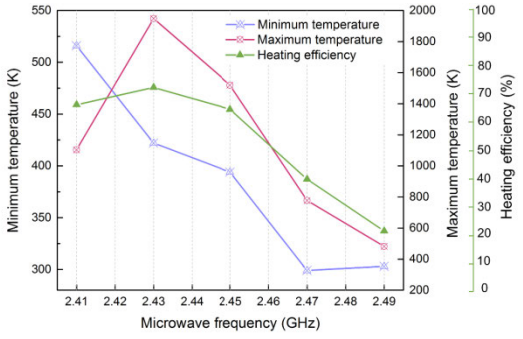

FIGURE 21. Effect of microwave frequency on heating efficiency and temperature.

Maximum temperature and electric field intensity increased rapidly when the frequency changed from 2.41GHz to 2.43GHz, shown in Fig.21. The region of hot and cold spots varied under different heating frequencies. The cold and hot spot was largest when frequency was 2.41GHz. The spot shrunk when the heating frequency increased. When the frequency continues to reach 2.45GHz, the maximum temperature and electric field intensity fall back. In the simulation, the maximum temperature and the largest difference temperature were occurred when frequency was 2.43GHz, which may cause more inhomogeneous expansion of sample and larger stress gradient. The relationship between maximum temperature, minimum temperature and microwave frequency did not present a certain law, which suggest that there is an optimal microwave heating frequency to achieve a more effective heating process under a typical heating circumstance.

Microwave heating efficiency could be indicated by the energy efficiency. In order to evaluate the energy efficiency quantitatively, the concept of microwave utilization efficiency was put forward, which could be expressed as:

$$\eta = \frac{P_a}{P_i} \times 100\% \tag{16}$$

where P_a is the absorbed power by sample (W), P_i is the total energy input (W).

The absorbed microwave power by sample as obtained by calculating the integration of internal energy through the microwave treatment and the total energy input were 1000W under the microwave frequency of 2.41, 2.43, 2.45, 2.47, 2.49 GHz, respectively. The green line in Fig.18 represent the heating efficiency varies with the microwave frequency. The maximum temperature and heating efficiency fluctuate with similar tendencies. For instance, the maximum temperature and highest energy efficiency occurred when the frequency was 2.43GHz. Higher microwave frequency does not definitely lead to higher energy efficiency. In the industrial application, a broader range of microwave frequency has been extended. Microwave frequency is directly related to the penetration depth, the effective heating frequency within in a wider range for different size of sample need to be investigated in further research.

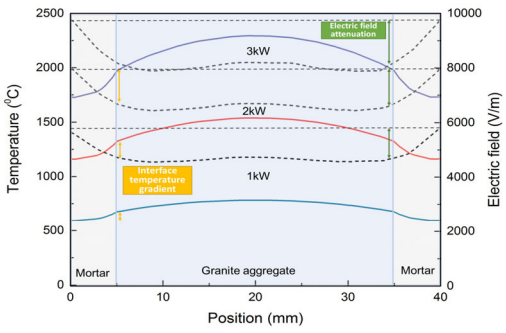

FIGURE 22. Electric and temperature field variation within mortar and aggregate.

E. INTERFACE EFFECT

The perspective of the research focus on the interface debonding of mortar and aggregate, that is the prerequisite of concrete aggregate recycling. The temperature and stress variation at the boundary were needed to be investigated. Fig.22 showed the electric and temperature field within mortar and aggregate under microwave heating power of 1kW, 2kW and 3kW. The dash line presents the electric field and the solid line presents the temperature variation. After 1 kW

microwave heating for 100s, the max and min electric field intensity were 5833V/m and 4554V/m, the max and min temperature were 782.2 °C and 563 °C, respectively.

It could be found that within the granite aggregate, electric field attenuation was occurred. As the microwave absorber, when microwave propagated through the granite and mortar, electromagnetic energy was transformed into heat energy, presenting as the electric field attenuation, resulting in temperature increase within granite. It could be found that higher microwave heating power lead to larger electric field attenuation and significant larger temperature difference at the interface, which may promote the interface debonding of mortar and aggregate.

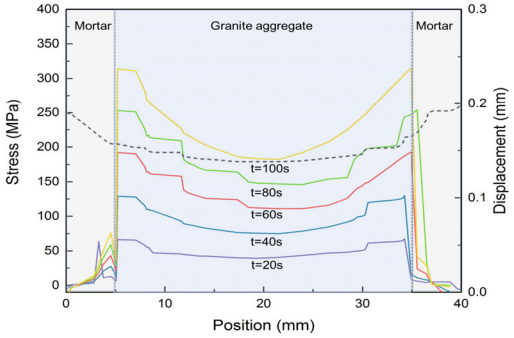

FIGURE 23. Radial stress variation within mortar and aggregate.

It could be found that there was stress mutation at the boundary of mortar and aggregate under microwave heating of 1kW, shown in Fig.23. The longer heating time, the larger stress gradient. The boundary debonding was formed based on the stress variation, which caused by stress difference and thermal expansion. The stress mutation at the interface could facilitate the debonding behavior. The black dash line showed the total displacement after 100s microwave irradiation. The larger displacement of mortar indicated the thermal expansion behaviors and the damage possibility of mortar matrix. Higher microwave power and longer heating time could lead to higher stress mutation between two materials, promoting the interface separation. The numerical results were corresponding with the experimental tests.

Fig. 24 presented the interface temperature gradient between mortar and aggregate under different microwave heating power varied with heating time. Two points were selected extremely near the boundary while one within aggregate phase and another in mortar matrix. The numerical results showed that with the increment of heating time and power, the temperature difference increased accordingly. After heating time of 100s under 5kW, the temperature gradient between mortar and aggregate reached about 200°C, which may contribute to easier interface debonding. The experimental results almost agree well with the numerical results except for temperature difference. The differences may due to the assumptions of the simulation model and the limitation of experiments.

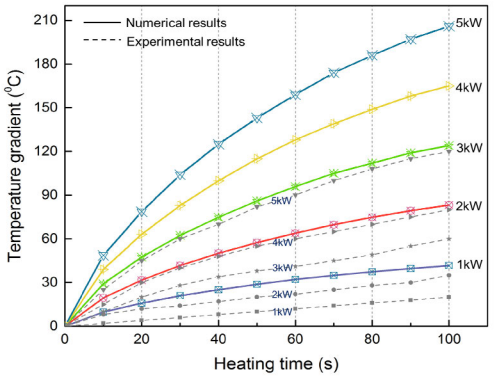

FIGURE 24. Mortar aggregate boundary temperature gradient.

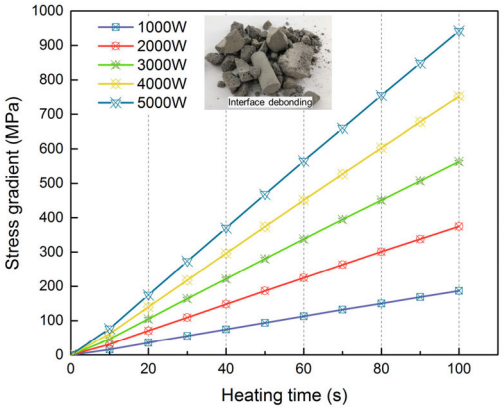

FIGURE 25. Stress gradient near mortar-aggregate interface.

The temperature difference leads to stress gradient between mortar and aggregate, shown in Fig.25. The dominant stress within mortar and aggregate were both tensile strengths. The boundary stress gradient increased with heating time and power input. The tensile strength within mortar lead to mortar damage and the stress gradient result in interface debonding. The experimental results proved that under higher microwave heating power, significant damage would occur within in mortar, and granite aggregate was separated from mortar matrix totally.

It could be concluded that the electric field variation and materials properties result in temperature gradient, leading to the stress difference at mortar and aggregate interface, promoting the interface debonding. Higher heating temperature filed and thermal expansion effect within mortar leading to the crack propagation throughout the mortar matrix and eventually the damage of mortar.

Fracture toughness is one of the material properties that defines the resistance of cracked materials (e.g., rocks, concrete) to deformation. Therefore, fracture toughness can be used as an index for micro-crack development in materials subjected to different loads. There are three basic modes of crack deformation under different stress regimes: Mode I (opening mode), Mode II sliding (in-phase shear) mode and

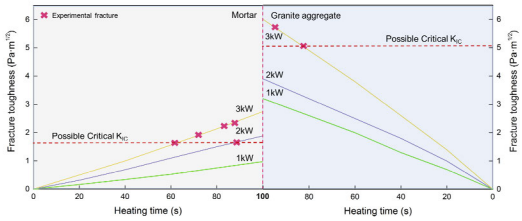

FIGURE 26. Evolution of fracture toughness of cracks within mortar and aggregate during microwave irradiation.

Mode III tearing (out-of-plane shear) mode [48]. The fracture toughness of pure Mode I is often considered as an intrinsic resistance to macroscopic fracturing in rocks [49]. Initial cracks within concrete caused by maximum tensile stress are more likely to extend rapidly and cause rock fracture. Fracture toughness of cracks under maximum tensile stress during the heating process is calculated according to Eq. 17:

$$K_{IC} = \sigma\sqrt{\pi a} \tag{17}$$

in which K_{IC} is the stress intensity factor of Mode I, that is fracture toughness (Pa·m$^{1/2}$), σ is stress loaded on crack surfaces (Pa), a is length of initial radial cracks (m). Initial crack length is assumed to be 50 μm. Fracture toughness of concrete under microwave heating power of 1kW, 2 kW and 3 kW within 100s was calculated, shown in Fig.26. The experimental fracture critical points were showed according to the tests results. The experimental fracture was defined as the apparent and observable damage occurred in mortar and aggregate. The intersection point of numerical results and experimental fracture may be the possible critical K_{IC}. The values of K_{IC} were larger than past experimental research, which may due to the experimental fracture used in comparison were the macro damage instead of the crack propagation. The region above the line of possible K_{IC} represent the condition that materials may occur damage. Although there were some assumptions and limitations for the calculation of K_{IC} under simulation process, the results could provide the reference and estimation of fracture condition of mortar and aggregate under microwave irradiation.

V. CONCLUSION

Prior work has achieved to give an insight into the complex multi-field coupling of microwave treatment process under various circumstance through the numerical simulation. Few researches investigated the concrete response subjected to microwave heating. In addition, these models did not consider the mass transfer process and mechanical field evolution with the sample.

In this paper, a multi-field coupling 3D simulation of concrete under microwave irradiation was carried out to analyze the heating process of concrete comprehensively. Four physical fields were employed in numerical simulation, the mechanical field, electromagnetic field, thermal field and mass transfer field to demonstrate the complex multi-field heating process of concrete under microwave irradiation. The response of aggregate and mortar under microwave irradiation and the interaction between the two materials were studied by a simplified concrete model. The heating responses of concrete were firstly analyzed, with the results of evolution of mechanical field, electromagnetic field, thermal field and mass transfer field concluded. The vital influence factors relating to the microwave heating were illustrated, including microwave heating frequency, power and time. The energy efficiency under different circumstances was calculated to achieve maximum utilization of microwave heating energy. This investigation could provide a comprehensive understanding of multi-field coupling and energy efficiency for the microwave assisted concrete recycling.

The following main conclusions can be obtained:

- Higher electromagnetic intensity lead to faster polarization effect, resulting in increment of heating temperature and thermal field. The distribution of temperature was corresponded to electromagnetic field. The longer the heating time, the larger temperature difference exhibited, the faster maximum temperature increased. Tensile stress was the dominate stress within the sample. Due to the difference of thermal and mechanics properties of two materials, a marked change of the principal stress was formed at the interface of mortar and granite. The tensile and shear stress were co-existed at the boundary of two materials, leading to the interface failure. The mortar may suffer damage firstly compared with granite, with larger deformation occurred under the microwave irradiation.
- The moisture concentration was directly relating to the temperature field within sample. The upper part of sample was heated more effectively due to the distribution of electromagnetic field. Compared with the moisture distribution within granite, the mortar's surface moisture could be easier evaporated and diffused as the host part.
- Under the equal microwave energy input, higher microwave power lead to higher maximum temperature and larger temperature difference within the sample. Higher microwave power level combined with shorter heating time may result in higher heating efficiency. Higher power could induce larger deformation per unit time.
- Temperature and stress gradient occurred near the interface mortar and aggregate, which may lead to interface debonding of mortar and aggregate. With the increment of heating time and power, the temperature and stress difference increased, promoting the interface separation accordingly.
- Microwave heating is highly sensitive to the heating frequency. Different microwave frequencies results in different electric field within the heating cavity and the sample, leading to the difference in the thermal and stress field. Energy efficiency various under different microwave frequency treatment. The variation law of maximum temperature and heating efficiency of sample was similar. The maximum temperature and

highest energy efficiency occurred when the frequency was 2.43GHz. Higher microwave frequency does not definitely lead to higher energy efficiency.

REFERENCES

[1] A. Buttress, A. Jones, and S. Kingman, "Microwave processing of cement and concrete materials–towards an industrial reality?" *Cement Concrete Res.*, vol. 68, pp. 112–123, Feb. 2015.

[2] N. Makul, P. Rattanadecho, and D. K. Agrawal, "Applications of microwave energy in cement and concrete–a review," *Renew. Sustain. Energy Rev.*, vol. 37, pp. 715–733, Sep. 2014.

[3] S. W. Kingman, "Recent developments in microwave processing of minerals," *Int. Mater. Rev.*, vol. 51, no. 1, pp. 1–12, Feb. 2006.

[4] W. Wei, Z. Shao, Y. Zhang, R. Qiao, and J. Gao, "Fundamentals and applications of microwave energy in rock and concrete processing–a review," *Appl. Thermal Eng.*, vol. 157, Jul. 2019, Art. no. 113751.

[5] S. W. Kingman and N. A. Rowson, "Microwave treatment of minerals—A review," *Minerals Eng.*, vol. 11, no. 11, pp. 1081–1087, Nov. 1998.

[6] K. Bru, S. Touzé, F. Bourgeois, N. Lippiatt, and Y. Ménard, "Assessment of a microwave-assisted recycling process for the recovery of high-quality aggregates from concrete waste," *Int. J. Mineral Process.*, vol. 126, pp. 90–98, Jan. 2014.

[7] Y. Menard, K. Bru, S. Touze, A. Lemoign, J. E. Poirier, G. Ruffie, F. Bonnaudin, and F. Von Der Weid, "Innovative process routes for a high-quality concrete recycling," *Waste Manage.*, vol. 33, no. 6, pp. 1561–1565, Jun. 2013.

[8] S. Liebezeit, A. Mueller, B. Leydolph, and U. Palzer, "Microwave-induced interfacial failure to enable debonding of composite materials for recycling," *Sustain. Mater. Technol.*, vol. 14, pp. 29–36, Dec. 2017.

[9] W. Wei, Z. Shao, R. Qiao, W. Chen, H. Zhou, and Y. Yuan, "Recent development of microwave applications for concrete treatment," *Constr. Build. Mater.*, to be published, doi: 10.1016/j.conbuildmat.2020.121224.

[10] M. G. Reddy, M. V. V. N. L. Sudharani, K. G. Kumar, A. J. Chamkha, and G. Lorenzini, "Physical aspects of Darcy–Forchheimer flow and dissipative heat transfer of Reiner–Philippoff fluid," *J. Thermal Anal. Calorimetry*, vol. 141, no. 2, pp. 829–838, Jul. 2020.

[11] M. G. Reddy, "Heat and mass transfer on magnetohydrodynamic peristaltic flow in a porous medium with partial slip," *Alexandria Eng. J.*, vol. 55, no. 2, pp. 1225–1234, Jun. 2016.

[12] G. R. Machireddy and S. Naramgari, "Heat and mass transfer in radiative MHD Carreau fluid with cross diffusion," *Ain Shams Eng. J.*, vol. 9, no. 4, pp. 1189–1204, Dec. 2018.

[13] S. A. Shehzad, M. G. Reddy, P. Vijayakumari, and I. Tlili, "Behavior of ferromagnetic Fe_2SO_4 and titanium alloy Ti_6Al_4v nanoparticles in micropolar fluid flow," *Int. Commun. Heat Mass Transf.*, vol. 117, Oct. 2020, Art. no. 104769.

[14] A. C. Metaxas and R. J. Meredith, *Industrial Microwave Heating*. Edison, NJ, USA: IET, 1983.

[15] D. M. Mingos and D. R. Baghurst, "ChemInform abstract: Applications of microwave dielectric heating effects to synthetic problems in chemistry," *ChemInform*, vol. 22, no. 36, pp. no–no, Aug. 2010.

[16] J. Figg, "Microwave heating in concrete analysis," *J. Appl. Chem. Biotechnol.*, vol. 24, no. 3, pp. 143–155, Apr. 2007.

[17] R. Qiao, Z. Shao, F. Liu, and W. Wei, "Damage evolution and safety assessment of tunnel lining subjected to long-duration fire," *Tunnelling Underground Space Technol.*, vol. 83, pp. 354–363, Jan. 2019.

[18] Y. Fernández, A. Arenillas, and J. Menéndez, *Microwave Heating Applied to Pyrolysis*. Oviedo, Spain: INTECH Open Access Publisher, 2011.

[19] G. Chen, J. Chen, S. Guo, J. Li, C. Srinivasakannan, and J. Peng, "Dissociation behavior and structural of ilmenite ore by microwave irradiation," *Appl. Surf. Sci.*, vol. 258, no. 10, pp. 4826–4829, Mar. 2012.

[20] G.-M. Lu, Y.-H. Li, F. Hassani, and X. Zhang, "The influence of microwave irradiation on thermal properties of main rock-forming minerals," *Appl. Thermal Eng.*, vol. 112, pp. 1523–1532, Feb. 2017.

[21] P. Hartlieb, M. Toifl, F. Kuchar, R. Meisels, and T. Antretter, "Thermo-physical properties of selected hard rocks and their relation to microwave-assisted comminution," *Minerals Eng.*, vol. 91, pp. 34–41, May 2016.

[22] P. Hartlieb, M. Leindl, F. Kuchar, T. Antretter, and P. Moser, "Damage of basalt induced by microwave irradiation," *Minerals Eng.*, vol. 31, pp. 82–89, May 2012.

[23] W. Li, M. A. Ebadian, T. L. White, R. G. Grubb, and D. Foster, "Heat and mass transfer in a contaminated porous concrete slab with variable dielectric properties," *Int. J. Heat Mass Transf.*, vol. 37, no. 6, pp. 1013–1027, Apr. 1994.

[24] N. Lippiatt and F. Bourgeois, "Investigation of microwave-assisted concrete recycling using single-particle testing," *Minerals Eng.*, vol. 31, pp. 71–81, May 2012.

[25] J. W. Walkiewicz, G. Kazonich, and S. L. McGill, "Microwave heating characteristics of selected minerals and compounds," *Minerals Metall. Process.*, vol. 5, no. 1, pp. 39-42, 1988.

[26] S.-H. Guo, G. Chen, J.-H. Peng, J. Chen, D.-B. Li, and L.-J. Liu, "Microwave assisted grinding of ilmenite ore," *Trans. Nonferrous Met. Soc. China*, vol. 21, no. 9, pp. 2122–2126, Sep. 2011.

[27] Y. Wang and N. Djordjevic, "Thermal stress FEM analysis of rock with microwave energy," *Int. J. Mineral Process.*, vol. 130, pp. 74–81, Jul. 2014.

[28] G. Wang, P. Radziszewski, and J. Ouellet, "Particle modeling simulation of thermal effects on ore breakage," *Comput. Mater. Sci.*, vol. 43, no. 4, pp. 892–901, Oct. 2008.

[29] S. Song, E. F. Campos-Toro, and A. López-Valdivieso, "Formation of micro-fractures on an oolitic iron ore under microwave treatment and its effect on selective fragmentation," *Powder Technol.*, vol. 243, pp. 155–160, Jul. 2013.

[30] E. Charikinya, S. Bradshaw, and M. Becker, "Characterising and quantifying microwave induced damage in coarse sphalerite ore particles," *Minerals Eng.*, vol. 82, pp. 14–24, Oct. 2015.

[31] M. Omran, T. Fabritius, and R. Mattila, "Thermally assisted liberation of high phosphorus oolitic iron ore: A comparison between microwave and conventional furnaces," *Powder Technol.*, vol. 269, pp. 7–14, Jan. 2015.

[32] M. Toifl, R. Meisels, P. Hartlieb, F. Kuchar, and T. Antretter, "3D numerical study on microwave induced stresses in inhomogeneous hard rocks," *Minerals Eng.*, vol. 90, pp. 29–42, May 2016.

[33] N. Makul, P. Rattanadecho, and A. Pichaicherd, "Accelerated microwave curing of concrete: A design and performance-related experiments," *Cement Concrete Compos.*, vol. 83, pp. 415–426, Oct. 2017.

[34] J. Huang, G. Xu, G. Hu, M. Kizil, and Z. Chen, "A coupled electromagnetic irradiation, heat and mass transfer model for microwave heating and its numerical simulation on coal," *Fuel Process. Technol.*, vol. 177, pp. 237–245, Aug. 2018.

[35] H. Zhu, J. He, T. Hong, Q. Yang, Y. Wu, Y. Yang, and K. Huang, "A rotary radiation structure for microwave heating uniformity improvement," *Appl. Thermal Eng.*, vol. 141, pp. 648–658, Aug. 2018.

[36] X. Gao, X. Liu, P. Yan, X. Li, and H. Li, "Numerical analysis and optimization of the microwave inductive heating performance of water film," *Int. J. Heat Mass Transf.*, vol. 139, pp. 17–30, Aug. 2019.

[37] H. Li, S. Shi, J. Lu, Q. Ye, Y. Lu, and X. Zhu, "Pore structure and multifractal analysis of coal subjected to microwave heating," *Powder Technol.*, vol. 346, pp. 97–108, Mar. 2019.

[38] Y.-D. Hong, B.-Q. Lin, H. Li, H.-M. Dai, C.-J. Zhu, and H. Yao, "Three-dimensional simulation of microwave heating coal sample with varying parameters," *Appl. Thermal Eng.*, vol. 93, pp. 1145–1154, Jan. 2016.

[39] B. Lin, H. Li, Z. Chen, C. Zheng, Y. Hong, and Z. Wang, "Sensitivity analysis on the microwave heating of coal: A coupled electromagnetic and heat transfer model," *Appl. Thermal Eng.*, vol. 126, pp. 949–962, Nov. 2017.

[40] J. Li, R. B. Kaunda, S. Arora, P. Hartlieb, and P. P. Nelson, "Fully-coupled simulations of thermally-induced cracking in pegmatite due to microwave irradiation," *J. Rock Mech. Geotechnical Eng.*, vol. 11, no. 2, pp. 242–250, Apr. 2019.

[41] L. F. Fan, Z. J. Wu, Z. Wan, and J. W. Gao, "Experimental investigation of thermal effects on dynamic behavior of granite," *Appl. Thermal Eng.*, vol. 125, pp. 94–103, Oct. 2017.

[42] W. Yao, K. Xia, and H.-W. Liu, "Influence of heating on the dynamic tensile strength of two mortars: Experiments and models," *Int. J. Impact Eng.*, vol. 122, pp. 407–418, Dec. 2018.

[43] A. Akbarnezhad, K. C. G. Ong, M. H. Zhang, C. T. Tam, and T. W. J. Foo, "Microwave-assisted beneficiation of recycled concrete aggregates," *Construct. Building Mater.*, vol. 25, no. 8, pp. 3469–3479, Aug. 2011.

[44] F. Zhang, J. Zhao, D. Hu, F. Skoczylas, and J. Shao, "Laboratory investigation on physical and mechanical properties of granite after heating and water-cooling treatment," *Rock Mech. Rock Eng.*, vol. 51, no. 3, pp. 677–694, Mar. 2018.

[45] P. Mounanga, A. Khelidj, and G. Bastian, "Experimental study and modelling approaches for the thermal conductivity evolution of hydrating cement paste," *Adv. Cement Res.*, vol. 16, no. 3, pp. 95–103, Jul. 2004.
[46] Y. S. Zhao, Z. J. Wan, Z. J. Feng, Z. H. Xu, and W. G. Liang, "Evolution of mechanical properties of granite at high temperature and high pressure," *Geomechanics Geophys. Geo-Energy Geo-Resour.*, vol. 3, no. 2, pp. 199–210, Jun. 2017.
[47] W. Wei, Z. Shao, P. Zhang, J. Cheng, and W. Chen, "Experimental study on thermal and mechanical behavior of mortar-aggregate under microwave irradiation," *J. Building Eng.*, to be published, doi: 10.1016/j.jobe.2020.101947.
[48] A. Mansourian, S. Hashemi, and M. R. M. Aliha, "Evaluation of pure and mixed modes (I/III) fracture toughness of portland cement concrete mixtures containing reclaimed asphalt pavement," *Construct. Building Mater.*, vol. 178, pp. 10–18, Jul. 2018.
[49] H. Qiu, Z. Zhu, M. Wang, F. Wang, Y. Ma, L. Lang, and P. Ying, "Study on crack dynamic propagation behavior and fracture toughness in rock-mortar interface of concrete," *Eng. Fract. Mech.*, vol. 228, Apr. 2020, Art. no. 106798.

WEI WEI was born in Yulin, Shaanxi, China, in 1992. She received the B.S. degree in civil engineering from the Xi'an University of Architecture and Technology, in 2014, and the M.S. degree in real estate from The University of Hong Kong, Hong Kong, in 2015. She is currently pursuing the Ph.D. degree with the Xi'an University of Architecture and Technology.

Her research interests include heat conduction in concrete materials, microwave heating in concrete and rock, and innovation process of concrete recycling.

Ms. Wei was a participant of the National Natural Science Foundation of China, in 2018, and the Found of Shaanxi Key Research and Development Program, in 2019.

ZHU-SHAN SHAO received the B.S. degree in mechanics from Lanzhou University, Lanzhou, China, in 1991, and the M.S. and Ph.D. degrees from Xi'an Jiaotong University, in 2000 and 2005, respectively.

From 2005 to 2006, he held a postdoctoral position with the National University of Singapore. Since 2009, he has been a Professor with the Xi'an University of Architecture and Technology. He is the author of more than 40 articles, and more than 30 inventions. His research interests include thermoelasticity, heat conduction, and mesomechanics in rock and concrete.

Prof. Shao was a recipient of the China National Natural Science Award (second class), in 2013.

WEN-WEN CHEN received the B.S. degree in civil engineering from the Xi'an University of Architecture and Technology, in 2018, where he is currently pursuing the M.S. degree.

His research interest includes microwave-assisted concrete recycling and curing.

Mr. Chen was a participant of the National Natural Science Foundation of China, in 2018, and the Found of Shaanxi Key Research and Development Program, in 2019.

PENG-JU ZHANG received the B.S. degree in civil engineering from the North China Institute of Science and Technology, in 2018. He is currently pursuing the master's degree with the Xi'an University of Architecture and Technology.

His research interests include microwave heating process in concrete and microwave-assisted aggregate recycling.

YUAN YUAN was born in Inner Mongolia, China, in 1993. She received the B.S. degree in civil engineering from the Xi'an University of Architecture and Technology, in 2014, where she is currently pursuing the Ph.D. degree.

Her research interests include microwave heating of rock and minerals, rock meso-mechanics, and microwave-assisted rock breaking. She was a participant of the National Natural Science Foundation of China, in 2018, and the Found of Shaanxi Key Research and Development Program, in 2019.